

Chapter 17

Advanced Topics

The detailed understanding of the onset of chaos via the period doubling cascade allows the calculation of many interesting quantities some measurable in experiment. Often the calculations involve considerable ingenuity, and described fully each would be a lecture in itself. Here, a selection of calculations are described briefly, and references to the original literature are given. Many of these references are available in the book by Cvitanović [1].

17.1 Chaotic behavior above the accumulation point

17.1.1 Qualitative description

Above the accumulation point of the period doubling bifurcations the dynamics consists of 2^n chaotic bands. There is completely regular jumping *between* the bands, but within each band the motion shows the characteristics of chaos and appears to be stochastic. The regular motion between the bands gives perfectly sharp peaks in the power spectrum; the chaotic motion within the bands adds a broad band background, and skirts to the peaks. The survival of the sharp peaks in the presence of the stochastic motion is reminiscent of the effect of thermal vibrations on X-ray peaks in crystallography: the thermal fluctuations do not lead to a cumulative uncertainty in the separation of atoms many lattice sites apart—each atom remains in the vicinity of the lattice site of the perfect crystal—and the X-ray peaks remain sharp. Similarly here, no matter how long the time delay, there is no uncertainty as to which band the iteration will lie in.

The bands successively merge at values of the map parameter with separations

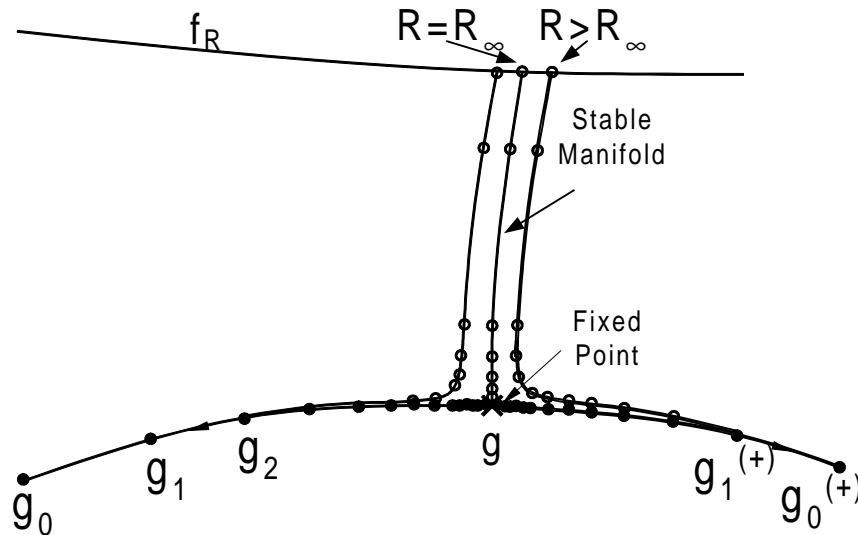


Figure 17.1: Renormalization group flows extended to include starting function above the onset of chaos.

that scale geometrically just as for $R < R_\infty$: the band merging of 2^n bands leading to 2^{n-1} bands occurs at values of $R_n^{(b)}$ given by

$$R_n^{(b)} - R_\infty = A^{(b)} \delta^{-n} \quad (17.1)$$

with δ the *same* number as in the scaling for $R < R_\infty$. It should be noted that many other phenomena occur between these values of R . For example periodic windows occur (the period 3 and period 5 windows are evident in the bifurcation plot, but in fact windows of any period occur), and these undergo their own infinite sequence of period doubling bifurcations. In fact near any parameter for which the dynamics is chaotic, there is a parameter value for which the orbit is periodic. The behavior is incredibly complicated and (17.1) focuses on just one aspect.

The qualitative aspects of the dynamics for the quadratic map for $a > a_c$ are shown in [demonstration 5](#).

17.1.2 RNG theory

The analog of the renormalization group theory for the period doubling bifurcations is to look at $T^n f_{R_n^{(b)}}$. At $R_n^{(b)}$ the dynamics hops between 2^n bands that are just

merging. Taking f^n strobes the dynamics so that successive iterations remain within a single band, and since the band is merging with its neighbors will just fill the band. The rescaling operation will expand this single band to fill the unit interval, and the final picture is reminiscent of the quadratic map at $a = 4$ where the chaos fills the unit interval. This is illustrated in [demonstration 6-8](#). In fact

$$\lim_{n \rightarrow \infty} T^n f_{R_n^{(b)}} = g_0^{(+)} \quad (17.2)$$

with $g_0^{(+)}$ the universal band filling chaotic map. As before, properties of the physical map can be related to universal properties of the map $g_0^{(+)}$ through the operation T [5],[6]. Again there is a whole sequence of universal function $g_m^{(+)}$. The flows are sketched in figure 17.1.

17.2 Higher Dimensions

What happens if higher dimensional maps are iterated? Is the fixed point still attracting, when the universality extends to higher dimensions, or does adding extra dimensions necessarily lead to extra unstable directions, when tuning a single parameter would not lead to the function crossing the critical surface in general? This is a crucial question for the relevance of the theory of period doubling bifurcations to physical systems, which are almost *never* described by a one dimensional map.

Collet, Eckmann, and Koch [4] showed that the universal period doubling behavior *may* survive in higher dimensions. (In fact they show that if the one parameter family of maps passes near the map (maybe after a coordinate transformation)

$$\begin{pmatrix} x_1 \\ x_2 \\ \vdots \\ x_N \end{pmatrix} \rightarrow \begin{pmatrix} g \left((x_1^2 - x_2 - \dots - x_N)^{1/2} \right) \\ 0 \\ \vdots \\ 0 \end{pmatrix} \quad (17.3)$$

with $g(x)$ the fixed point function then the “transverse directions” contract more rapidly than the α^{-1} scaling of the one dimensional map, (in fact as α^{-2}) and the fixed point structure survives.)

Whether a particular example of a higher dimensional map will satisfy this criterion (after sufficient functional composition etc.) is much harder to calculate,

and the occurrence of the period doubling sequence is almost always only known empirically. Similarly, it is very hard to predict whether a given physical system will show the period doubling route to chaos. Usually we must be satisfied with empirical evidence: if, say, period doubling up to period 64 is observed, then it is likely that this behavior is controlled by the “period doubling fixed point”—why else would so many period doubling bifurcations occur—and then it is likely that the full sequence to chaos will be observed.

The Hénon map is a simple example that shows a period doubling cascade. Remember the map is

$$\begin{aligned} x_{n+1} &= y_n + 1 - ax_n^2 \\ y_{n+1} &= bx_n \end{aligned} \quad (17.4)$$

As $b \rightarrow 0$, and in as much as the quadratic map at its critical value is “close to $g(x)$ ” this falls into the form demanded by Collet, Eckman and Koch. We can alternatively write the map as

$$x_{n+1} = 1 - ax_n^2 + bx_{n-1} \quad (17.5)$$

which for small b is well approximated by the quadratic map. Defining $\bar{a} = 1 + \sqrt{1 + 4a}$ and transforming $x = X\bar{a}/a$ and taking $b \rightarrow 0$ gives

$$X_{n+1} = -\frac{1}{2} + \bar{a} \left(\frac{1}{2} - X_n^2 \right) \quad (17.6)$$

the form of the quadratic map with the maximum at $X = 0$. Note also that y_n provides a record of x_{n-1} so that the plot of the Hénon map will directly mimic the plot of the quadratic map. Thus for small b we expect the period doubling route to chaos. In fact this continues to hold for the “standard” value $b = 0.3$. This is illustrated in [demonstrations 1-4](#). A crude estimate from these demonstrations gives the values of a for the transitions

$n \rightarrow n + 1$	a_n	$a_n - a_{n-1}$	$\frac{a_n - a_{n-1}}{a_{n-1} - a_{n-2}}$
2 \rightarrow 4	0.912		
4 \rightarrow 8	1.027	.115	
8 \rightarrow 16	1.051	.024	4.8
16 \rightarrow 32	1.0565	.005	4.8

(17.7)

showing the rough agreement with the expected ratio of $\delta = 4.67$.

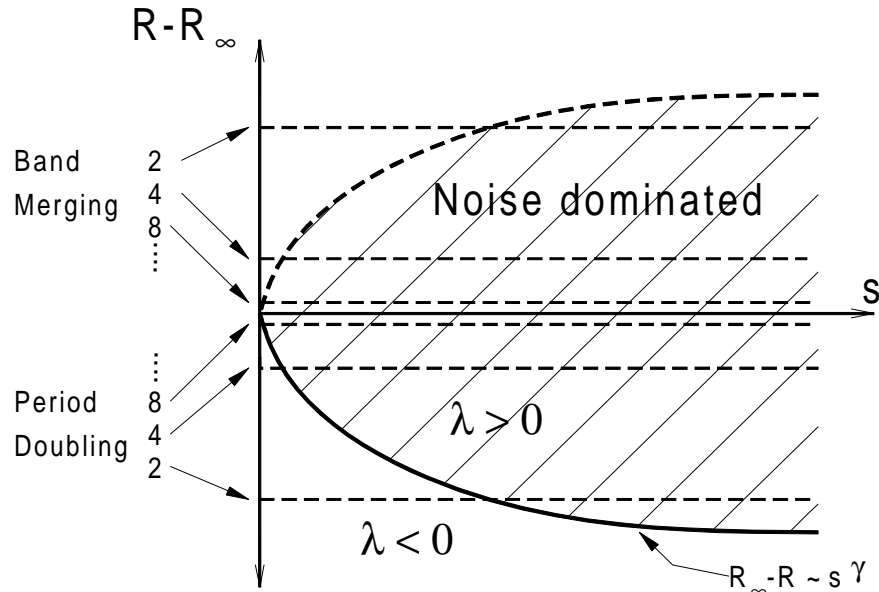


Figure 17.2: Effect of noise on the period doubling route to chaos.

17.3 Added noise

The addition of stochastic noise to the map dynamics acts like an additional field at a thermodynamic transition—for example the magnetic field at the phase transition to a ferromagnet. Intuitively we would expect the transition to be “rounded” with high order 2^n -cycles eliminated by the noise, and with a broad band component of the power spectrum always present. In addition we might expect the transition to chaos to occur earlier.

The addition of small amplitude noise of strength s can be treated quantitatively and has interesting scaling properties. The results are derived below and summarized in figure (17.2). The onset of chaos, marked by a positive Lyapunov exponent, is enhanced by an amount $R_\infty - R \sim s^\gamma$ with the exponent $\gamma \simeq 0.82$. In addition the region $|R_\infty - R| \sim s^\gamma$ can be described as noise dominated: within this range, for example, successive orbit or band splittings are eliminated by the noise.

We now derive these results (for more details see Crutchfield et al. [7]). With

the noise the map dynamics becomes

$$x_{n+1} = \bar{f}(x_n) = f(x_n) + s\xi_n, \quad (17.8)$$

where ξ_n is randomly $\pm\frac{1}{2}$ and s is the small noise strength. The first step of functional composition now takes the form

$$\begin{aligned} \bar{f}(\bar{f}(x)) &= f(\bar{f}(x)) + s\xi' \\ &= f(f(x)) + f'(f(x))s\xi'' + s\xi' \end{aligned} \quad (17.9)$$

and since ξ' and ξ'' are the noises at successive steps and are therefore independent, they add in quadrature so that

$$\bar{f}(\bar{f}(x)) = f(f(x)) + s(x)\xi \quad (17.10)$$

and we see that an x dependent noise strength $s(x)$ is generated:

$$s(x) = s\sqrt{1 + (f'(f(x)))^2}. \quad (17.11)$$

If we suppose f is at the accumulation point in the absence of noise, then successive functional composition and rescaling will bring the map to the vicinity of the fixed point $g(x)$, but we expect the noise term to eventually lead to divergence from the fixed point. Again we linearize about the fixed point and look at maps

$$\bar{f} = g + s\xi D(x) \quad (17.12)$$

where $sD(x)$ is the x -dependent noise and we look for the eigenvector $D(x)$ and associated eigenvalue K so that

$$T[\bar{f}] = g + Ks\xi D(x). \quad (17.13)$$

Performing the functional composition as in (17.9)

$$\bar{f}(\bar{f}(x)) = g(g(x)) + s\xi \left\{ [g'(g(x))D(x)]^2 + [D(g(x))]^2 \right\}^{1/2} \quad (17.14)$$

and adding the rescaling leads to the eigenvalue equation

$$\alpha \left\{ [g'(g(x))D(x)]^2 + [D(g(x))]^2 \right\}^{1/2} = KD(\alpha x). \quad (17.15)$$

A simple polynomial approximation to D gives $K \simeq 6.619$.

There are now *two* unstable directions at the fixed point, given by $h(x)$ important when $R \neq R_\infty$, and by $D(x)$ important with added noise. This is analogous to a magnetic transition where the two unstable direction correspond to temperature and magnetic field. We get two parameter scaling as is found in that case. For example consider the case again of the Lyapunov exponent. The basic scaling of the Lyapunov exponent is unchanged by the noise

$$\lambda[\bar{f}] = \frac{1}{2^n} \lambda[T^n \bar{f}]. \quad (17.16)$$

However putting in the two unstable directions leads to

$$\lambda[\bar{f}_{R_m}, s] = \frac{1}{2^n} \lambda[T^{n-p} [g + \delta^{p-m} h(x) + B_s K^p D(x)]], \quad (17.17)$$

where we have in addition to the growth at the rate δ along $h(x)$ (c.f. equation (16.24)), growth along $D(x)$ with initial amplitude proportional to the noise strength s . Now we take $m = n \rightarrow \infty$ with $n - p = q$ fixed

$$\lambda[\bar{f}_{R_n}, s] = \frac{1}{2^n} \lambda[T^q [g + \delta^{-q} h(x) + B_s K^{-q} K^n D(x)]] \quad (17.18)$$

For $K = 0$ this is the construction that led to $2^{-n} \lambda[g_0]$. Absorbing universal quantities into the definition of a scaling function Φ_1 we get

$$\lambda[\bar{f}_{R_n}, s] = 2^{-n} \Phi_1(A_1 s K^n), \quad (17.19)$$

where A_1 involves the unknown B and so is nonuniversal, but Φ_1 is a universal function (explicitly $\Phi_1(y)$ is the Lyapunov exponent of the map function

$$T^q [g(x) + \delta^{-q} h(x) + K^{-q} D(x) y] \quad (17.20)$$

which is universal because q is a chosen value, and g , h and D are universal functions defined by the properties of the fixed point).

As before it is useful to rewrite the dependence on n in terms of $R_\infty - R_n = c\delta^{-n}$ using

$$\begin{aligned} K^n &= \delta^{n/\gamma} \propto (R_\infty - R_n)^{-1/\gamma} \\ 2^n &= \delta^{n/\beta} \propto (R_\infty - R_n)^{-\beta} \end{aligned} \quad (17.21)$$

with

$$\gamma = \frac{\log \delta}{\log K} \simeq 0.815 \quad \text{and} \quad \beta = \frac{\log 2}{\log \delta}. \quad (17.22)$$

Then we can write an expression for the dependence of λ on the control parameter R and the noise strength s

$$\lambda(R, s) = A_2 (R_\infty - R)^\beta \Phi_2 \left(A_3 \frac{s}{(R_\infty - R)^{1/\gamma}} \right) \quad (17.23)$$

where Φ_2 is a universal function simply related to Φ_1 , and A_2, A_3 are nonuniversal amplitudes. As usual it is understood that this relationship applies at a sequence of R giving the same type of orbit (superstable, bandmerging etc). This is a typical *two scale factor scaling relationship*, and the behavior depends how the limits $s \rightarrow 0, R_\infty - R \rightarrow 0$ are taken. For example, for zero noise strength (17.23) reproduces the no noise result $\lambda(R, s) \propto (R_\infty - R)^\beta$ (where $\Phi_2(0)$ is included in the proportionality constant). However we see that noise becomes important for strength $s \sim |R_\infty - R|^{1/\gamma}$.

Sometimes a slightly different form of the scaling relationship is useful: write $\Phi_2(y) = y^\beta \Phi_3(y^{-\gamma})$ to give

$$\lambda(R, s) = A_4 s^u \Phi_3 (A_5 s^{-\gamma} (R_\infty - R)) \quad (17.24)$$

with

$$u = \beta\gamma = \frac{\log 2}{\log K} \simeq 0.34. \quad (17.25)$$

The scaling equation (17.24) tells us that if we plot $s^{-u} \lambda [f_{R_n}, s]$ against $s^{-\gamma} (R_\infty - R_n)$ then after we have used the freedom to fix the x and y axis scales (the non-universal constants A_4, A_5) the points should lie on a *single curve* for all noise strengths s, R_n and map functions. In addition we can pick off various limits:

1. For zero noise strength as we have seen

$$\lambda [R, s = 0] \propto |R_\infty - R|^\beta. \quad (17.26)$$

2. For $R = R_\infty$ we must have

$$\lim_{x \rightarrow 0} \Phi_3(x) = \text{const} \quad (17.27)$$

and then

$$\lambda [R_\infty, s] \propto s^u. \quad (17.28)$$

3. The onset of chaos where λ changes sign occurs for $\Phi_3(x) = 0$ i.e. for some particular value of x . This then shows $\lambda = 0$ for

$$R_\infty - R_n \propto s^\gamma. \quad (17.29)$$

The proportionality constant is found to be positive, so the onset of chaos is *enhanced* by the addition of noise of strength s , by an amount proportional to $s^{0.82}$, and at the old onset position λ has a value that scales as $s^{0.34}$. These are the results leading to figure 17.2.

17.4 Separation of points in orbit

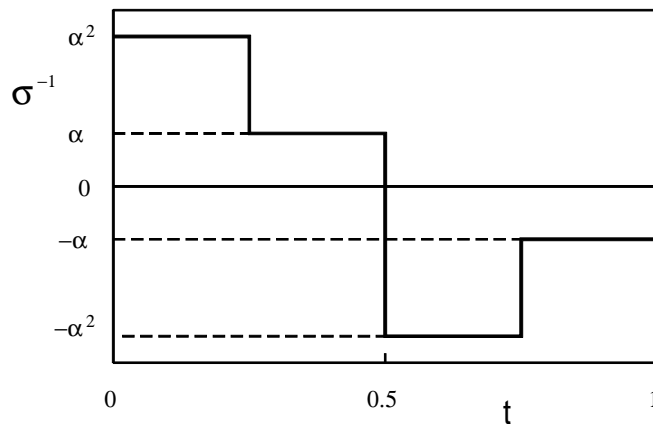


Figure 17.3: A crude plot of the splitting function $\sigma(t)$: the inverse of the splitting σ^{-1} is plotted as a function of the fraction around the orbit t .

The basic scaling in the definition of T corresponds to the observation that for the superstable 2^n cycles the separation between the point at the maximum and the nearest point in the cycle (which is given by iterating half way around the cycle i.e. 2^{n-1} times) shrinks as n increases like α^{-n} . However the scaling of adjacent points is not uniform around the cycle. For example if we iterate these neighboring points separated by d_n once, we get points separated by d_n^2 , since the points are iterated through the quadratic maximum. Thus the separation of these adjacent points scale as $(\alpha^2)^{-n}$. In fact the decrease in separation with n can be expressed in terms of

a universal function σ of the fractional distance around the orbit. The function σ is complicated (in fact discontinuous at every rational), and its derivation is quite intricate, and is discussed only briefly here. Often it is sufficient to approximate $|\sigma|$ roughly by α^{-1} over half the range and α^{-2} over the other half: this crude approximation is shown in figure (17.3). For more details and an accurate plot see Feigenbaum's article [2].

More generally we define the separation scaling function $\sigma_n(t)$ as

$$\sigma_n(t) = \frac{d_{n+1}(m)}{d_n(m)} \quad \text{with} \quad t = \frac{m}{2^{n+1}}. \quad (17.30)$$

and

$$\sigma(t) = \lim_{n \rightarrow \infty} \sigma_n(t)$$

Thus $\sigma_n(t)$ gives the ratio of the separation of adjacent points a number of m iterations from the point at the maximum as a function of the fraction around the orbit t . Precisely we can identify

$$d_n \equiv d_n(0) = f_{R_n}^{2^{n-1}}(x_0) - x_0 \quad (17.31)$$

where x_0 is the coordinate of the maximum which is zero for the shifted coordinate used in the renormalization procedure. But we can evaluate this easily in terms of the universal functions for large n

$$d_n = (-\alpha)^{-(n-1)} g_1(0). \quad (17.32)$$

Similarly

$$d_{n+1} = f_{R_{n+1}}^{2^n}(0) - 0 = (-\alpha)^{-n} g_1(0) \quad (17.33)$$

so that

$$\sigma(0) = \lim_{n \rightarrow \infty} \sigma_n(0) = -\alpha \quad (17.34)$$

which is the basic scaling result.

We can begin to investigate the dependence on t by the same procedure for a point $m = 2^{n-r}$ iterations around the orbit. Then

$$d_n(m) = f_{R_n}^{2^{n-r}}(0) - f_{R_n}^{2^{n-r}} f_{R_n}^{2^{n-1}}(0) \quad (17.35)$$

since again we iterate 2^{n-1} times around the orbit from the starting point (itself given by iterating 2^{n-r} times from the maximum) to find the closest point. Relating the functional composition to the operation T and hence introducing the universal map functions g gives for large m, n

$$d_n(m) = (-\alpha)^{-(n-r)} \left[g_r(0) - g_r \left((-\alpha)^{-(r-1)} g_1(0) \right) \right]. \quad (17.36)$$

Similarly $d_{n+1}(m)$ is given by an expression with the same prefactor (since m and so $n - r$ is fixed) but increasing $r \rightarrow r + 1$ in the []. This then gives

$$\sigma(t = 2^{-r-1}) = \frac{g_{r+1}(0) - g_{r+1} \left((-\alpha)^{-r} g_1(0) \right)}{g_r(0) - g_r \left((-\alpha)^{-(r-1)} g_1(0) \right)}. \quad (17.37)$$

Although already complicated, this is not the whole story, since not all points around the orbit are given by a fraction of the form $t = 2^{-r}$. More generally we must look at the binary expansion of the fraction $t = 2^{-r_1} + 2^{-r_2} + \dots$, which leads to an even more complicated expression, that can however be constructed in terms of the g_i . This leads to a $\sigma(t)$ with the following properties:

- $\sigma(t + \frac{1}{2}) = -\sigma(t)$;
- it is universal, and given by the g_i ;
- $|\sigma|$ is roughly α^{-1} over half the range and α^{-2} over the other half, but is in fact discontinuous at every rational.

17.5 Power Spectrum

Successive period doubling bifurcations bring in subharmonic peaks in the spectrum due the small splitting of points from the orbit before the bifurcation. The splitting is given by d_n and the power spectrum can be calculated from the knowledge of this quantity. A full calculation is quite involved (see Feigenbaum [2] or Schuster's book for more details), but since this is an important diagnostic tool, and was important in the historical verification of the theory, the first steps are presented here.

For the 2^n cycle the amplitude of the k th peak at frequency $\omega_k = 2\pi k/2^n$ is given by

$$a_k^n = \frac{1}{2^n} \sum_{j=0}^{2^n-1} \exp \left[-\frac{2\pi i k j}{2^n} \right] x(j). \quad (17.38)$$

For k odd (corresponding to the peaks that were *not* present at the $(n - 1)$ th level) we can sum over half the cycle, and then include the second half explicitly

$$\begin{aligned} a_k^n &= \frac{1}{2^n} \sum_{j=0}^{2^{n-1}-1} \exp\left[-\frac{2\pi i k j}{2^n}\right] [x(j) - x(j + 2^{n-1})], \\ &= \frac{1}{2^n} \sum_{j=0}^{2^{n-1}-1} \exp\left[-\frac{2\pi i k j}{2^n}\right] d_n(j). \end{aligned} \quad (17.39)$$

(For k even, the second half of the cycle would contribute with a positive sign in the first of these expressions.) We can write down a similar expression for a_k^{n+1} which will depend on the $d_{n+1}(j) = \sigma_n(j/2^n)d_n(j)$. However extracting the features of the power spectrum that depend just on the universal function σ remains intricate. As a *very* rough guide we first ignore the j dependence of the d_n . Then for k odd

$$|a_k^{n+1}| \simeq \frac{1}{2^{n+1}} \cot\left(\frac{\omega_k}{4}\right) d_{n+1} \quad (17.40)$$

with a similar expression for $|a_k^n|$. Thus we have at the new peaks

$$|a^{n+1}(\omega)| \simeq \frac{1}{2} \frac{d_{n+1}}{d_n} |a^n(\omega)| \quad (17.41)$$

where by $a^n(\omega)$ we mean (since at the n th level there was no peak at this value of frequency!) the interpolated value from the peaks that are present. To take into account the variation of d_{n+1} around the orbit, a better (but still approximate) calculation shows that the correct evaluation of the ratio d_{n+1}/d_n is the mean square splitting factor around the orbit $\sqrt{\frac{1}{2}(\alpha^{-2} + \alpha^{-4})}$ (using the two value approximation to σ). This then gives

$$\left|a_{2m+1}^{n+1}\right| \simeq \mu^{-1} \left|a_{(2m+1)/2}^n\right| \quad \text{with} \quad \mu \simeq \frac{1}{2} \sqrt{\frac{1}{2}(\alpha^{-2} + \alpha^{-4})} \simeq 0.1525. \quad (17.42)$$

which is a 16.3dB decrease in the power $|a(\omega)|^2$ for successive subharmonics in the spectrum. The approximate scaling of the power spectrum was verified experimentally by Libchaber and Maurer [3] in their experiment on convection in mercury.

The scaling of the power spectrum of the chaotic bands above the onset of chaos can be calculated using similar arguments. The power in the broad band component of the power spectrum is given by the scaling function σ , since at each band merging the dynamics is reproduced scaled by this function. If P_n is the power

at the 2^n band merging point, then again making the two-value approximation to σ

$$\frac{P_{n+1}}{P_n} = \beta^2 \simeq \frac{1}{2} \left(\frac{1}{\alpha^2} + \frac{1}{\alpha^4} \right) \simeq 10.8. \quad (17.43)$$

Alternatively we can write this as

$$P_n \propto \left(R_n^{(b)} - R_\infty \right)^{\bar{\gamma}}$$

with $\bar{\gamma} \simeq \log \beta^2 / \log \delta \simeq 1.54$.

February 23, 2000

Bibliography

- [1] P. Cvitanović, “Universality in Chaos” (2nd Edition, IOP, Bristol 1989)
- [2] M.J. Feigenbaum, *J. Stat. Phys.* **21**, 669 (1979)
- [3] A. Libchaber and J. Maurer, *J. Phys. (Paris) Coll.* **41**, C3 (1980)
- [4] P. Collet and J.-P. Eckmann, “Iterated Maps of the Interval as Dynamical Systems”, (Birkhauser, Boston)
- [5] M. Nauenberg and J. Rudnick, *Phys. Rev.* **B24**, 493 (1981)
- [6] A. Wolf and J. Swift, *Phys. Lett.* **83A**, 184 (1981)
- [7] J. Crutchfield, M. Nauenberg, and J. Rudnick, *Phys. Rev. Lett.* **46**, 933 (1981)